Published in final edited form as:

Magn Reson Imaging. 2023 October ; 102: 133–140. doi:10.1016/j.mri.2023.05.003.

Fetal-placental MR angiography at 1.5 T and 3 T

Feifei Qu, PhD[1], **Taotao Sun, MD**[2,3,4,*], **Julio Marin-Concha, MD**[4,5], **Sunil Jaiman, MD**[5,6], **Ling Jiang**[2,3], **Swati Mody, MD**[7], **Edgar Hernandez-Andrade, MD, PhD**[4,5], **Karthikeyan Subramanian, MS**[1], **Zhaoxia Qian, MD**[2,3], **Roberto Romero, MD, DMedSci**[5,8,9,10,11,12], **E. Mark Haacke, PhD**[1,13,*]

[1]Department of Radiology, Wayne State University School of Medicine, Detroit, Michigan, USA

[2]Department of Radiology, International Peace Maternity and Child Health Hospital, School of Medicine, Shanghai Jiao Tong University, Shanghai, China

[3]Shanghai Key Laboratory of Embryo Original Diseases, Shanghai, China

[4]Department of Obstetrics and Gynecology, Wayne State University School of Medicine, Detroit, Michigan, USA

[5]Perinatology Research Branch, Division of Obstetrics and Maternal-Fetal Medicine, Division of Intramural Research, *Eunice Kennedy Shriver* National Institute of Child Health and Human Development, National Institutes of Health, U.S. Department of Health and Human Services, Bethesda, Maryland, and Detroit, Michigan, USA

[6]Department of Pathology, Wayne State University School of Medicine, Detroit, Michigan, USA

[7]Department of Radiology, Children Hospital of Michigan, Detroit, Michigan, USA

[8]Department of Obstetrics and Gynecology, University of Michigan, Ann Arbor, Michigan, USA

[9]Department of Epidemiology and Biostatistics, Michigan State University, East Lansing, Michigan, USA

[10]Center for Molecular Medicine and Genetics, Wayne State University, Detroit, Michigan, USA;

[11]Detroit Medical Center, Detroit, Michigan, USA

[*]**Corresponding Authors:** *Taotao Sun and E. Mark Haacke have contributed equally to this work.* Taotao Sun, MD, Department of Radiology, International Peace Maternity and Child Health Hospital, School of Medicine, Shanghai Jiao Tong University, Shanghai, China. taotaosun_mri@126.com; phone: +86-13917117665. E. Mark Haacke, PhD, Department of Radiology, Wayne State University School of Medicine, 4201 St. Antoine, Detroit, MI, 48201, USA. nmrimaging@aol.com; phone: 313-745-1395, fax: 313-745-9182.

CRediT authorship contribution statement

Feifei Qu: Conceptualization, Methodology, Software, Formal analysis, Investigation, Data curation, Writing – original draft, Visualization.

Taotao Sun: Methodology, Data curation, Writing – original draft, Writing – review & editing, Project administration.

Julio Marin-Concha: Formal analysis, Investigation, Writing – original draft, Writing– review & editing.

Sunil Jaiman: Writing – original draft, Writing –review & editing.

Ling Jiang: Methodology, Data curation, Writing –original draft.

Swati Mody: Conceptualization, Methodology, Data curation, Writing – original draft, Writing – review & editing.

Edgar Hernandez-Andrade: Investigation, Writing – review & editing.

Karthikeyan Subramanian: Data curation, Writing – review & editing.

Zhaoxia Qian: Conceptualization, Resources, Supervision, Funding acquisition.

Roberto Romero: Conceptualization, Methodology, Validation, Writing – review & editing, Supervision, Resources, Funding acquisition, Project administration.

E. Mark Haacke: Conceptualization, Methodology, Validation, Writing – review & editing, Supervision.

[12]Department of Obstetrics and Gynecology, Florida International University, Miami, Florida, USA

[13]Department of Biomedical Engineering, College of Engineering, Wayne State University, Detroit, Michigan, USA.

Abstract

Objectives: The objective of this work was to investigate the application of 2D Time-of-Flight (TOF) magnetic resonance angiography (MRA) to observe the placental vasculature at both 1.5T and 3T.

Methods: Fifteen appropriate for gestational age (AGA) (GA: 29.7 ± 3.4 weeks; GA range: 23 and 6/7 weeks to 36 and 2/7 weeks) and eleven patients with an abnormal singleton pregnancy (GA: 31.4 ± 4.4 weeks; GA range: 24 weeks to 35 and 2/7 weeks) were recruited in the study. Three AGA patients were scanned twice at different gestational ages. Patients were scanned either at 3T or 1.5T using both T_2-HASTE and 2D TOF to image the entire placental vasculature.

Results: The umbilical vessels, chorionic vessels, stem vessels, arcuate arteries, radial arteries, and spiral arteries were shown in most of the subjects. Hyrtl's anastomosis was found in two subjects in the 1.5 T data. The uterine arteries were observed in more than half of the subjects. For those patients scanned twice, the same spiral arteries were identified in both scans.

Conclusions: 2D TOF is a technique that can be applied in studying the fetal-placental vasculature at both 1.5T and 3T.

Keywords

Magnetic resonance angiography; Placental vasculature; Hyrtl's anastomosis

1. Introduction

The placenta is a fundamental organ that plays an important role in the nutrition supply and respiration of the fetus, supporting normal fetal development throughout the pregnancy [1]. Placental flow and oxygen supply to the tissue increases across gestational age as does blood flow in the arteries and intervillous space [2–4]. The endometrial blood supply of non-pregnant women changes from a few millimeters per minute to 500 millimeters per minute in pregnant women at term [5]. The continuous distension of the uteroplacental arteries during the 2nd and 3rd trimester causes an increase of blood supply favorable to the growth of the placenta and the fetus [6]. To date, 3D/4D ultrasound (US) and spatiotemporal image correlation have been used clinically to evaluate the fetal vasculature [7–9]. However, US is limited by the small field of view (FOV), cross sectional resolution, the presence of bony structures, abnormal fetal position, and maternal obesity.

Magnetic resonance angiography (MRA) is a powerful tool to evaluate tissue vasculature and, in the case of imaging the placental vasculature, could be a valuable accessory to US imaging. Some studies have evaluated the use of MR imaging in ex-vivo studies of the placenta using a contrast agent [10–12]. Our previous study showed that in vivo imaging of the placenta without a contrast agent can be accomplished using a conventional MRA approach based on 2D time-of-flight (TOF) imaging to generate both placental and fetal

vasculature [13]. That study was done using a 3T scanner (Verio, Siemens, Erlangen, Germany), and all the experiments were performed in the late 3rd trimester. Although currently more centers are trying to use 3T for imaging the fetus, the majority of studies still take place at 1.5 T during both the 2nd and 3rd trimesters. Therefore, our goal was to investigate the feasibility of using 2D TOF MRA in the placenta and the fetus at both 1.5T and 3T in the 2nd and the 3rd trimesters.

2. Materials and Methods

This cross-sectional study was conducted at two facilities. Fifteen of the patients were recruited from the Center for Advanced Obstetric Care and Research Perinatology Research Branch of the Eunice Kennedy Shriver National Institute of Child Health and Human Development (NICHD), National Institutes of Health, Wayne State University School of Medicine, Hutzel Women's Hospital in conjunction with the Magnetic Resonance Research Facility, Wayne State University, and the Detroit Medical Center, Detroit, Michigan U.S.A. The other eleven patients were recruited from the Department of Radiology, International Peace Maternity and Child Health Hospital (IPMCH), School of Medicine, Shanghai Jiao Tong University, Shanghai, China. All patients recruited in the U.S.A. provided written informed consent for both ultrasound and MRI examinations and were enrolled in research protocols approved by the Human Investigation Committee of Wayne State University and the Institutional Review Board of the NICHD. All patients recruited in China provided written informed consent for both ultrasound and MRI examinations and were enrolled in research protocols approved by the IPCMH Human Investigation Committee compliant with HIPAA regulations.

2.1 Patient Population

A total of 15 patients with appropriate for gestation age (AGA) pregnancy with estimated fetal weight between the 10th and 90th percentile (GA: 29.7 ± 3.4 weeks; GA range: 23 and 6/7 weeks to 36 and 2/7 weeks) and 11 patients with an abnormal singleton pregnancy (GA: 31.4 ± 4.4 weeks; GA range: 24 weeks to 35 and 2/7 weeks) had MR imaging and were included in the study. Six AGA subjects (GA: 29.0 ± 3.0 weeks; GA range: 23 and 6/7 weeks to 32 and 3/7 weeks) and five abnormal cases (GA: 28.9 ± 4.8 weeks; GA range: 24 weeks to 33 and 5/7 weeks) were performed at 1.5 T, and nine AGA subjects (GA: 30.0 ± 3.7 weeks; GA range: 23 and 6/7 weeks to 36 and 2/7 weeks) and six abnormal cases (GA: GA: 33.4 ± 3.1 weeks; GA range: 27 and 1/7 weeks to 35 and 2/7 weeks) were performed at 3T. Three AGA subjects were scanned twice with the first scan in the 2nd trimester and the second one in the 3rd trimester six to nine weeks apart at 3T. The clinical conditions diagnosed by the last MRI/US before the study and the MRI scanner used in the study for all the subjects are listed in Table 1. Gestational age was confirmed with an early ultrasound scan in all patients. It is worth noting that the pathology tests of subject No. 19 and subject No. 21 after delivery were both normal, and the abnormalities of subject No. 2 and subject No. 6 were unlikely to be affected by placental development. Therefore, all these four subjects were classified as AGA.

2.2 Data Acquisition

MRI studies were performed on a 3T Siemens Verio system (Erlangen, Germany) with a 6-channel flex coil and a 4-channel spine coil, or on a 1.5T Siemens Aera MRI system (Erlangen, Germany) with an 18-channel body coil and a 12-channel spine coil. The patients were placed in a supine or lateral decubitus position based on their preference during the scan. The first part of the imaging protocol consisted of an initial scout sequence followed by a multi-slice T_2-Half-Fourier Single Shot Turbo Spin Echo (HASTE) sequence both with a FOV covering the entire organ. The T_2-HASTE images were used as a reference for the 2D TOF angiography sequences. The parameters of the 2D TOF sequence are given in Table 2. The sequence was performed twice under the following two circumstances: (1) the images contained significant motion artifact or (2) the image SNR was too low because of the patients' large body size. This situation only occurred for patients recruited in the 3 T study. In the latter case, a lower resolution image would be collected if the high resolution scan generated low SNR image. The 3D reconstruction was performed using SPIN software (SpinTech MRI, Bingham Farms, USA), and the vascular network visualization was processed in 3D using VolView [14].

2.3 Image quality evaluation

All images were reviewed by two radiologists (TS and LJ) both with more than 5 years of clinical experience in fetal MR imaging. The TOF image quality was evaluated using a 5-point scale and a 2-point scale, with higher scores indicating better image quality (Table 4). Cohen's Kappa coefficient was calculated to estimate the inter-observer agreement between two readers.

3. Results

Several example MR angiograms are shown in Fig. 1 for five subjects. The fetal-placental vasculature, including chorionic vessels and stem vessels, is clearly demonstrated (Fig. 1-d). Hyrtl's anastomosis was seen in two subjects (Fig. 1e). To better demonstrate the connection between the two umbilical arteries (UAs), the umbilical vein (UV) in the first case shown in Fig. 1e was manually cropped and removed. The UAs and UVs were easily visualized in all subjects. The maternal-placental vasculature, including the ascending uterine arteries, the arcuate arteries in the placenta basal plate, and the connected radial arteries, can also be observed (Fig. 1f–g). The entire vascular system is clearly shown in one of the IUGR cases collected at 3 T (Fig. 2) [15]. The uterine arteries were only found in 14 cases by the first reader and 21 cases by the second reader (Table 3). Both readers agreed that for the rest of the cases, more slices would be needed to distinguish the uterine artery from the iliac artery. This is because only the placental region was fully covered during the scanning to reduce the scan time. Radial arteries and the connected spiral arteries were identified in most of the cases, and one subject with hydrocephalus is shown in Fig. 3. Five spiral arteries were observed from this subject (Fig. 3b–f). The UVs and UAs are labeled to serve as a reference to localize the spiral arteries. The different vessels that could be identified for all subjects and the image quality score results are given in Table 3. Three AGA subjects were recruited twice at 3 T, once in the 2nd trimester and once in the 3rd trimester. From the various spiral arteries observed in the first scan for these three cases, eight were successfully identified in

both scans (Fig. 4 and Fig. 5). The inter-observer agreement of the image quality is listed in Table 4. The 5-point score generated moderate agreement while the 2-point score generated substantial agreement.

4. Discussion

In this work, we showed that for the majority of subjects scanned, whether at 1.5 T or 3 T, most of the major maternal-placental vessels can be visualized. The umbilical and arcuate arteries were observed in the MRA data for all patients while the chorionic and some stem, spiral, and radial arteries could be seen in most of the subjects. For those subjects with repeated scans at different trimesters, the same radial and spiral arteries could be identified from scan to scan. In two cases, Hyrtl's anastomosis could be seen. Many of these vessels could be viewed in their entirety on 3D rendering. Both normal subjects and patients with different types of abnormality were recruited in the study; the ability of the 2D TOF MRA to display the placental vascular network was not affected by the patients' clinical conditions.

The image quality of most subjects was diagnostically acceptable. The reason for the poor image quality in three of the subjects was twofold: either severe motion artifact (even after repeat scanning) or poor SNR due to the subject's large body size and insufficient coil coverage. Therefore, motion artifacts and SNR were the two main culprits leading to poor image quality. Generally, by limiting the slice coverage to just the placenta, the scan time was kept to a reasonable level and less than 10% of the slices, if any, showed motion artifact. In this study, there were 6 subjects with a BMI of more than 30 recruited, and all of them were performed at 3 T. In most cases, the image quality was improved by using the faster low resolution scan (change from 0.5×0.5 mm^2 to 1.0×1.0 mm^2). Only one of them generated low SNR images. Finally, a better set of coils could improve the image quality and solve this SNR problem.

Since the placenta supplies the nutrients to the fetus, it is critical that the vasculature and blood flow to and from the fetus at normal levels for both the placenta and fetus develop properly. The chorionic plate provides the flow to the fetus while the basal plate contains the maternal vessels [16]. Each placental lobe is formed by several cotyledons in close contact with each other, and there are 10 to 40 cotyledons in a normal placenta [16]. The cotyledons represent the terminal segment of the fetal circulation [17]. The presence and general location of the different maternal and fetal side vessels is well known [4]. The chorionic plate vessels form around 60 to 70 primary villous stem vessels which later divide into secondary and tertiary vessels [18]. Each primary stem vessel ends in a fetal cotyledon [19]. Anomalies of the placental vasculature have been associated with different maternal and fetal conditions such as preeclampsia, fetal growth restriction, diabetes mellitus, and congenital heart disease [11, 20]. In normal subjects, Rasmussen et al. reported that the fetal size correlated to the placental vascular density [10]. In another study on fetal growth restriction (FGR), Link et al showed a strong correlation between placental volume, vascular volume, and gestational age [11].

Placental vasculature in FGR cases demonstrated differences in size and structure of the vessels (such as tortuosity of the terminal villi and branching angle) when compared

with normal placentas [21]. Also, ex-vivo studies demonstrated differences in the vascular volume and length of fetal vessels in cases of FGR [21–23]. Janaid et al reported that the median vessel length was shorter in arterial placental vessels in cases of FGR in comparison with normal placentas by using micro CT [23]. These ex-vivo studies required the use of contrast agents or exposure to radiation during imaging. With faster imaging and better resolution, 2D TOF MRA could well become a practical clinical tool to investigate the vascular distribution in the placenta during pregnancy. Higher resolution will benefit the study of smaller vessels affecting placental development, such as the radial, spiral and stem vessels. Hyrtl's anastomosis could also be seen by 2D TOF MRA. In a previous study, it was found that the width of Hyrtl's anastomosis was related to the degree of placental symmetry with respect to the size of the supplying areas of the umbilical arteries [24].

Another potential application of mapping the major vessels in the placenta relates to the blood circulation in each cotyledon including the vasculature in the basal plate and the cotyledon itself. From the basal plate, the oxygenated blood from the maternal side passes through the arcuate arteries and is delivered to the intervillous space via the radial arteries which transform into the spiral arteries. Oxygen and nutrients from the intervillous space are extracted at the level of vasculosyncytial membranes (VSM) in the terminal villi. The oxygen and nutrient rich blood traverses out from the terminal villous capillary network into the postcapillary venule of the terminal villous, which is in turn connected with the postcapillary type venule in the mature intermediate villous and stem villous. The stem villous venule ascends into the chorionic plate. These chorionic plate veins coalesce and form the UV (Supplemental material Fig. 1).

There are several limitations to this work. First, only vessels with sufficiently rapid through plane flow will be seen. To overcome this limitation, a second and potentially third scan could be run orthogonal to the first to capture in-plane vessels from the first scan. Second, it is worth noting that image resolution, contrast and SNR are key to visualize small vessels such as the radial and spiral arteries. A higher resolution of 0.5 mm × 0.5 mm × 2.0 mm could help resolve smaller vessels and better utilize vessel tracking algorithms. This will require excellent SNR and rapid imaging methods. Rapid imaging methods such as radial imaging [25, 26] and Controlled Aliasing in Parallel Imaging Results in Higher Acceleration (CAIPRIHAINA) could lead to further speed improvements of 2 to 4 opening the door to practical higher resolution imaging [27]. The third limitation comes from motion induced breathing artifacts. Along these lines, even without motion artifacts per slice, motion of the placenta between slices (that is motion on the order of a 5 to 10 second time period) could cause some shifting of the vessels from slice to slice. However, this was generally not a major problem for the placenta. If this were to remain a problem, it could potentially be resolved using vessel tracking techniques to re-register the vessels [28].

5. Conclusions

In conclusion, 2D TOF is a technique that can be used to study the placental vasculature at both 1.5T and 3T. It can reveal all major placental vessels throughout the placenta, making it possible, in principle, to study local deficits of blood flow. Future improvements in speed

and image quality and in enhancing the small vessels could lead to an even better delineation of the radial, spiral, and stem vessels.

Supplementary Material

Refer to Web version on PubMed Central for supplementary material.

Acknowledgment

This research was supported, in part, by the Perinatology Research Branch, Division of Obstetrics and Maternal-Fetal Medicine, Division of Intramural Research, *Eunice Kennedy Shriver* National Institute of Child Health and Human Development, National Institutes of Health, U.S. Department of Health and Human Services (NICHD/NIH/DHHS); and, in part, with Federal funds from NICHD/NIH/DHHS under Contract No. HHSN275201300006C. Dr. Roberto Romero has contributed to this work as part of his official duties as an employee of the United States Federal Government.

Abbreviations:

MRA	Magnetic resonance angiography
TOF	Time-of-Flight
AGA	Appropriate for gestational age
GA	Gestational age
HASTE	Half-Fourier Single Shot Turbo Spin Echo
UV	Umbilical vein
UA	Umbilical artery

Reference

1. Turco MY, Moffett A. Development of the human placenta. 2019 Nov 15;146(22):dev163428.
2. Burton GJ, Jauniaux E. Pathophysiology of placental-derived fetal growth restriction. Am. J. Obstet. Gynecol 2018 Feb 1;218(2):S745–S761. [PubMed: 29422210]
3. Rodesch F, Simon P, Donner C, Jauniaux E. Oxygen measurements in endometrial and trophoblastic tissues during early pregnancy. Obstet. Gynecol 1992 Aug 1;80(2):283–285. [PubMed: 1635745]
4. Ramsey EM. Maternal and foetal circulation of the placenta. Ir. J.Med. Sci 1971 Apr;140(4):151–168. [PubMed: 4997466]
5. Browne JCM, Veall N. The maternal placental blood flow in normotensive and hypertensive women. BJOG: An International Journal of Obstetrics and Gynaecology. 1953 Apr;60(2):141–147.
6. Robertson WB. Uteroplacental vasculature. j. Clin, Pathol. Supplement (Royal College of Pathologists). 1976;10:9
7. Gonçalves LF, Romero R, Espinoza J et al. Four-dimensional ultrasonography of the fetal heart using color Doppler spatiotemporal image correlation. J Ultrasound Med. 2004 Apr;23(4):473–481. [PubMed: 15098864]
8. Gonçalves LF, Lee W, Chaiworapongsa T et al. Four-dimensional ultrasonography of the fetal heart with spatiotemporal image correlation. Am. J. Obstet. Gynecol 2003 Dec 1;189(6):1792–1802. [PubMed: 14710117]
9. Yagel S, Cohen SM, Shapiro I, Valsky DV. 3D and 4D ultrasound in fetal cardiac scanning: a new look at the fetal heart. Ultrasound Obstet. Gynecol.: The Official Journal of the International Society of Ultrasound in Obstetrics and Gynecology. 2007 Jan;29(1):81–95.

10. Rasmussen AS, Stæhr-Hansen E, Lauridsen H, Uldbjerg N, Pedersen M. MR angiography demonstrates a positive correlation between placental blood vessel volume and fetal size. Arch. Gynecol. Obstet 2014 Dec;290(6):1127–1131. [PubMed: 25033715]
11. Link D, Many A, Ben-Sira L et al. Placental vascular tree characterization based on ex-vivo MRI with a potential application for placental insufficiency assessment. Placenta. 2020 Jul 1;96:34–43. [PubMed: 32560856]
12. Rasmussen AS, Lauridsen H, Laustsen C et al. High-resolution ex vivo magnetic resonance angiography: a feasibility study on biological and medical tissues. BMC Physiol. 2010 Dec;10(1):1–8 . [PubMed: 20113508]
13. Neelavalli J, Krishnamurthy U, Jella PK, et al. Magnetic resonance angiography of fetal vasculature at 3.0 T. Eur. Radiol 2016 Dec;26(12):4570–4576. [PubMed: 27189488]
14. Ibanez L, Schroeder W, Ng L, Cates J. The ITK Software Guide, Kitware. Inc. Clifton Park, New York. 2005.
15. Sørensen A, Sinding M, Peters DA et al. Placental oxygen transport estimated by the hyperoxic placental BOLD MRI response. Rhysiol. Rep 2015 Oct;3(10):e12582.
16. Benirschke K, Burton GJ, Baergen RN. Pathology of the Human Placenta, 6th edn. Berlin: Springer; 2012.
17. Barker D, Osmond C, Grant S et al. Maternal cotyledons at birth predict blood pressure in childhood. Placenta. 2013 Aug 1;34(8):672–675. [PubMed: 23731799]
18. Benirschke K, Kaufmann P, Baergen RN. Pathology of the Human Placenta, 5th edn. New York : Springer-Verlag; 2006.
19. Wigglesworth JS. Vascular anatomy of the human placenta and its significance for placental pathology. BJOG: An International Journal of Obstetrics and Gynaecology. 1969 Nov;76(11):979–989.
20. Thunbo MØ, Sinding M, Bogaard P et al. Postpartum placental CT angiography in normal pregnancies and in those complicated by diabetes mellitus. Placenta. 2018 Sep 1;69:20–25. [PubMed: 30213480]
21. Haeussner E, Schmitz C, Frank HG, Von Koch FE. Novel 3D light microscopic analysis of IUGR placentas points to a morphological correlate of compensated ischemic placental disease in humans. Sci. Rep 2016 Apr 5;6(1):1–11. [PubMed: 28442746]
22. Langheinrich AC, Vorman S, Seidenstücker J et al. Quantitative 3D micro-CT imaging of the human feto-placental vasculature in intrauterine growth restriction. Placenta. 2008 Nov 1;29(11):937–41. [PubMed: 18851884]
23. Junaid TO, Bradley RS, Lewis RM, Aplin JD, Johnstone ED. Whole organ vascular casting and microCT examination of the human placental vascular tree reveals novel alterations associated with pregnancy disease. Sci. Rep 2017 Jun 23;7(1):1–10. [PubMed: 28127051]
24. Ullberg U, Sandstedt B, Lingman G. Hyrtl's anastomosis, the only connection between the two umbilical arteries. A study in full termplacentas from AGA infants with normal umbilical artery blood flow. Acta Obstet. Gynecol. Scand 2001 Jan 1;80(1):1–6 [PubMed: 11167180]
25. Yadav BK, Krishnamurthy U, Jella PK et al. Radial Segmented Echo-Planar Readout for Fast Fetal Angiography – Feasibility Test. In: Proceedings of the Joint Annual Meeting ISMRM-ESMRMB. Honolulu, USA 4818; 2017.
26. Krishnamurthy U, Yadav BK, ella PK et al. In-utero non-contrast MR angiography of the fetal vasculature using a double-echo radial sampling scheme. In: Proceedings of the Joint Annual Meeting ISMRM-ESMRMB. Honolulu, USA 0103; 2017.
27. Breuer FA, Blaimer M, Mueller MF et al. Controlled aliasing in volumetric parallel imaging (2D CAIPIRINHA). Magn. Reson. Med 2006 Mar;55(3):549–556. [PubMed: 16408271]
28. Buch S, Wang Y, Park MG et al. Subvoxel vascular imaging of the midbrain using USPIO-Enhanced MRI. NeuroImage. 2020 Oct 15;220:117106.

Key points:

The placental vasculature can be visualized using 2D TOF MRA at both 1.5T and 3T.

The spiral artery could be reproducibly identified at different gestational ages by MRA.

Hyrtl's Anastomosis can be identified in MRA.

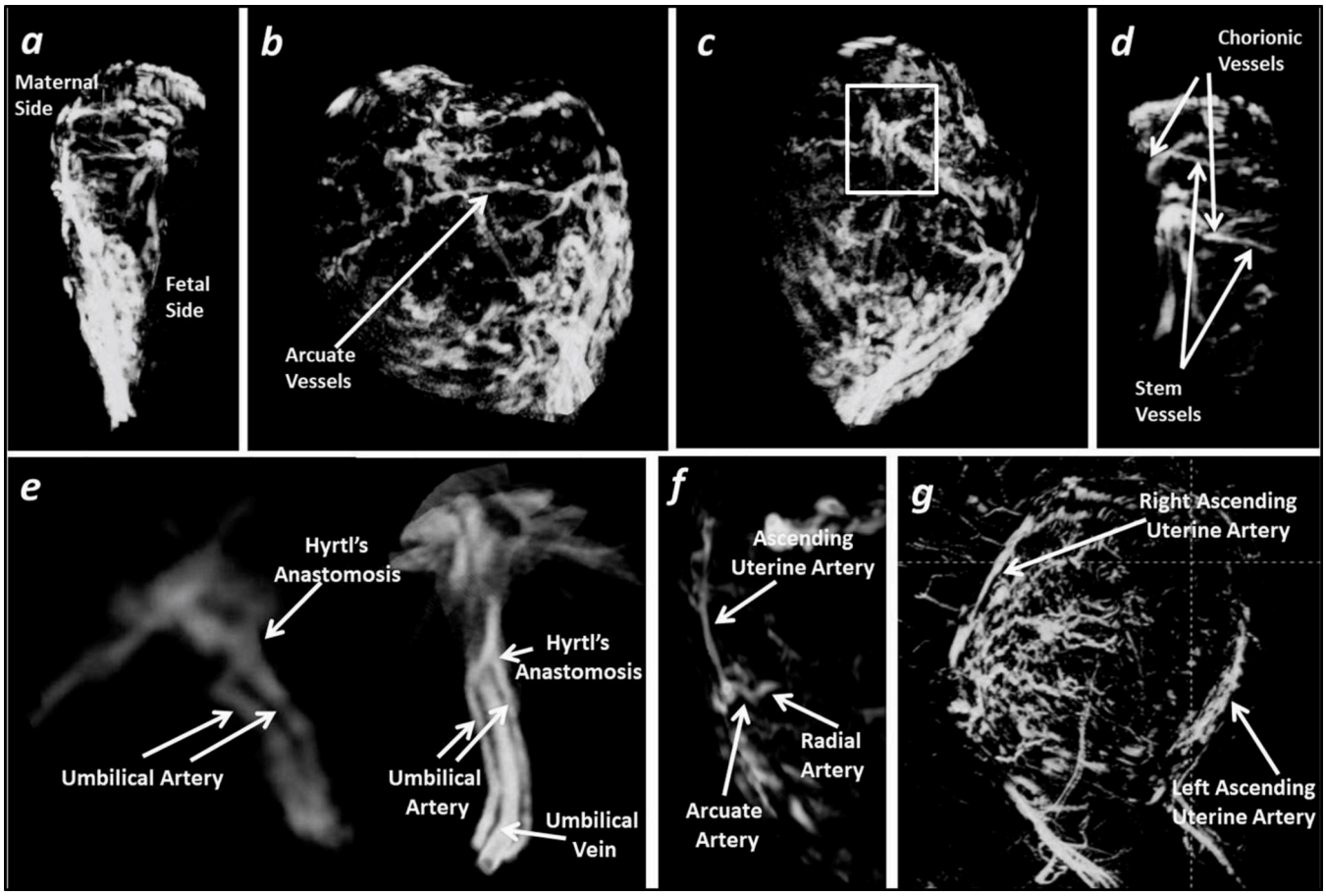

Fig 1.

Placental vasculature. Normal subject No. 1, data collected at 3T with high resolution. a) Sagittal view of the placenta MRA; b) Arcuate vessels can be identified at the surface of the placenta; c) and d) Chorionic vessels and the connected stem vessels inside the placenta can be clearly identified. Abnormal subjects No. 2 and No. 3, data collected at 1.5 T. e) UV, UAs, and the Hyrtl's anastomoses were displayed. Normal subject No. 4, data collected at 1.5 T. f) Ascending uterine artery, arcuate artery and radial artery can be visualized. Normal subject No. 5, data collected at 3T with low resolution. g) The right ascending uterine artery and the left ascending uterine artery are visible.

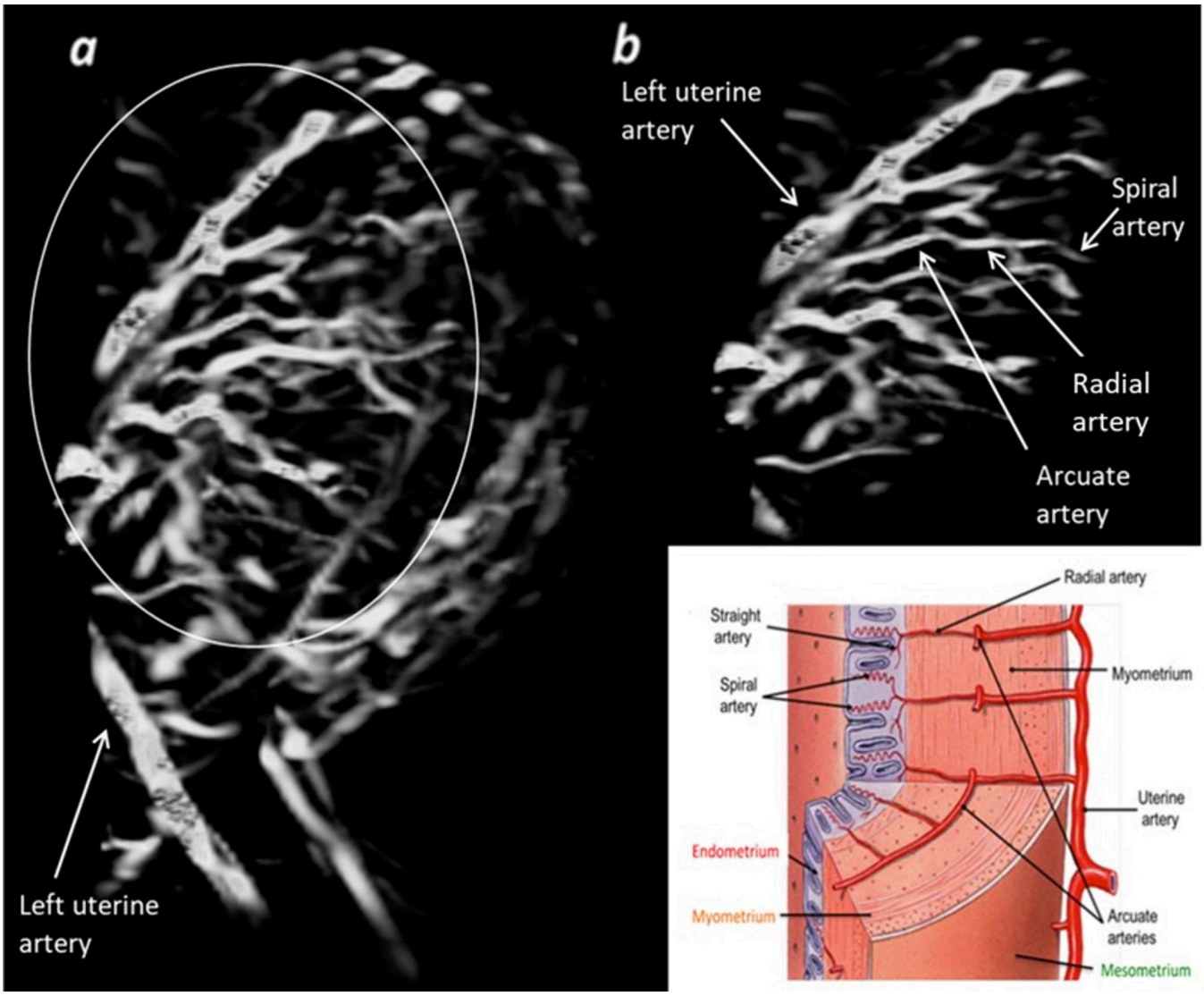

Fig 2.

Maternal-placental vasculature and the arcuate system. IUGR subject No. 26, data collected at 3T with high resolution. a) Sagittal 3D view of the placenta; b) The ascending uterine artery branching out into the arcuate system and further into the radial and spiral arteries.

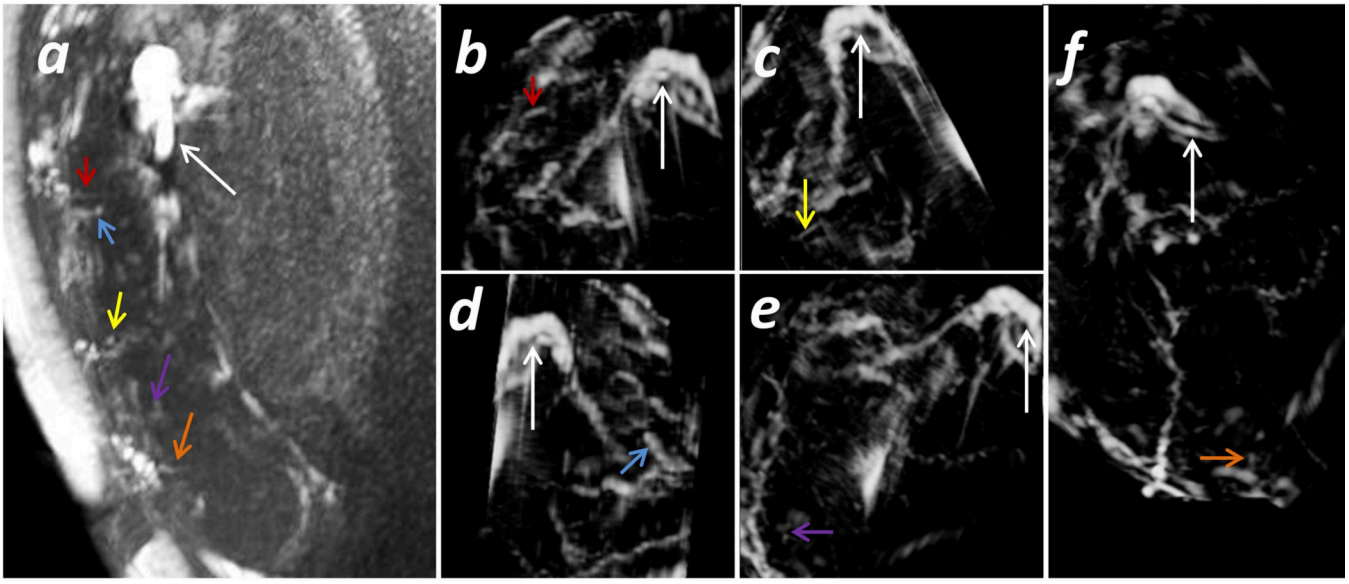

Fig 3.

Spiral arteries inside the placenta. Subject No. 6: A subject with hydrocephalus collected at 1.5 T. a) A single 2D slice from the TOF images with the 3D MIP; b-f) MRA of a single spiral artery in part of the placental vasculature at different orientations. The UV and UAs are marked by the white arrows. The spiral arteries are marked by the colored arrows. The arrows with the same color mark the same spiral artery in the different images.

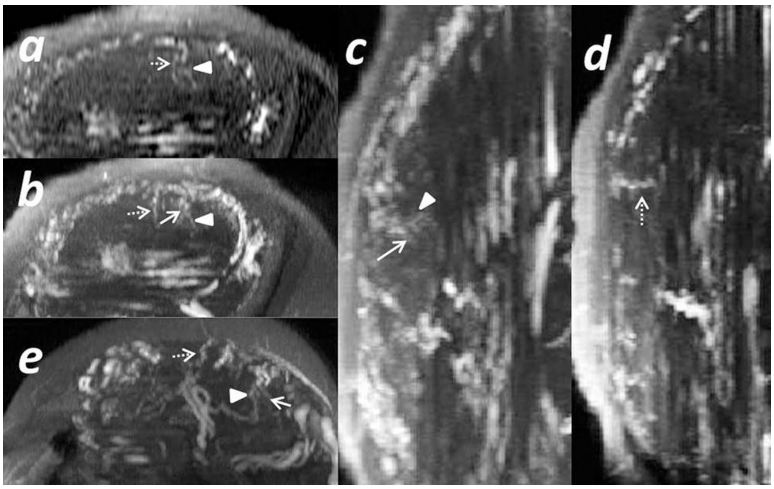

Fig 4.

Spiral arteries identified in two scans. Subject 5: A normal subject collected at 3 T with low resolution. The first scan was performed at 23 + 6/7 weeks: a) A single 2D slice from the TOF image for the axial view; b) TOF image with the 3D MIP for the axial view; c) and d) TOF images with the 3D MIP for the sagittal view. The second scan was performed at 33 + 3/7 weeks: e) TOF image with the 3D MIP for the axial view. The same stem vessel is marked by an arrowhead, and two different spiral arteries found in both scans are marked with a solid and dashed arrow, respectively.

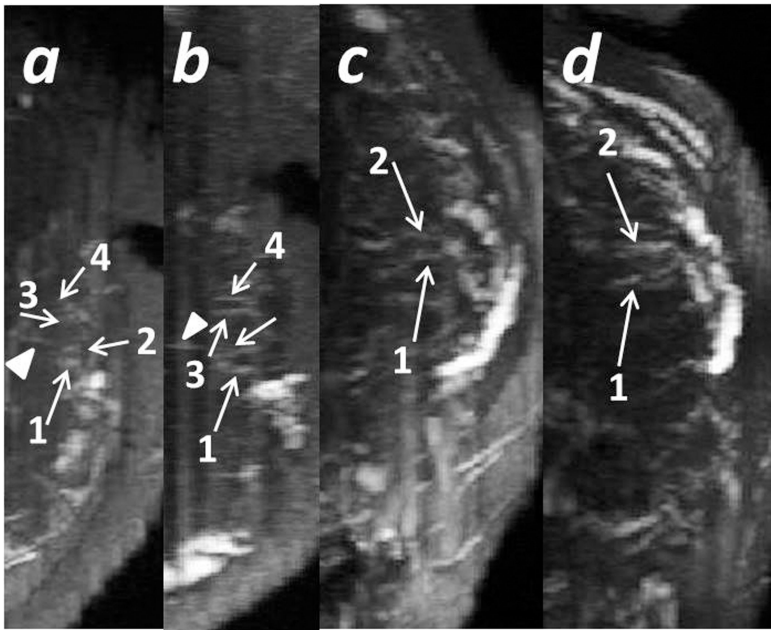

Fig 5.

The spiral arteries identified in two scans from two subjects. Subject No.7: A normal subject collected at 3 T with low resolution. A single 2D slice from the TOF image with the 3D MIP for the axial view collected in the first scan a) and the second scan b). Subject No.8: A normal subject collected at 3 T with low resolution. A single 2D slice from the TOF image with the 3D MIP for the axial view collected in the first scan c) and the second scan d). The same stem vessel is marked by an arrowhead. Spiral arteries are marked with arrows. The same spiral arteries see in both scans are marked by the same numbers.

Table 1.

Clinical condition and the MRI scanner for all subjects

Subject No.	**1**		**2**		**3**		**4**		**5**		**6**	
Clinical Condition	Normal		Widening of lateral ventricles		IUGR		Normal		Normal		Hydrocephalus	
GA (weeks)	36 + 2/7		29		33 + 5/7		23 + 6/7		1st: 23 + 6/7, 2nd: 33 + 3/7		28 + 2/7	
MRI scanner	3 T		1.5 T		1.5 T		1.5 T		3 T		1.5 T	
Placenta Position	A		A		P		P		P		A	
BMI	50.19		23.80		24.68		25.39		1st: 20.12 2nd: 30.54		22.66	
Reader	No.1	No.2	No.1	No.2	No.1	No.2	No.1	No.2	No.1	No.2	No.1	No.2
Radial Arteries												
Spiral Arteries												
Ascending Uterine arteries												
Image Quality	4	4	5	5	5	5	4	4	5	5	5	4
Subject No.	**7**		**8**		**9**		**10**				**11**	
Clinical Condition	Normal		Normal		Normal		Normal				IUGR	
GA (weeks)	1st: 27 + 4/7, 2nd: 33 + 6/7		1st: 25 + 6/7, 2nd: 32 + 3/7		32 + 3/7		30 + 5/7				33 + 3/7	
MRI scanner	3 T		3 T		1.5 T		3 T				1.5 T	
Placenta Position	A		A		P		A				A	
BMI	1st: 31.55, 2nd: 31.37		1st: 20.66, 2nd: 21.31		24.69		24.94				27.4	
Reader	No.1	No.2	No.1	No.2	No.1	No.2	No.1		No.2		No.1	No.2
Radial Arteries												
Spiral Arteries												
Ascending Uterine arteries												
Image Quality	4	3	4	4	4	3	2		2		3	5
Subject No.	**12**		**13**		**14**		**15**				**16**	
Clinical Condition	Placental chorioangioma		IUGR		Normal		Normal				Normal	
GA (weeks)	29 + 2/7		35 + 1/7		30 + 3/7		28 + 1/7				33 + 1/7	
MRI scanner	1.5 T		3 T		3 T		3 T				3 T	
Placenta Position	A		A		A		A				A	
BMI	24.39		24.8		28.53		35.11				26.04	
Reader	No.1	No.2	No.1	No.2	No.1	No.2	No.1		No.2		No.1	No.2

Subject No.	**1**		**2**		**3**		**4**		**5**		**6**	
Radial Arteries												
Spiral Arteries												
Ascending Uterine arteries												
Image Quality	4	5	3	5	3	3	4		4		5	4
Subject No.	**17**		**18**		**19**		**20**				**21**	
Clinical Condition	Marginal umbilical cord insertion		Normal		Low-lying placenta		Thickening of placenta in US				Low-lying placenta	
GA (weeks)	24 + 1/7		26 + 1/7		31 + 4/7		24				28 + 6/7	
MRI scanner	1.5 T		3 T		1.5 T		1.5 T				1.5 T	
Placenta Position	P		A		P		P				P	
BMI	23.64		28.51		24.61		25.08				24.58	
Reader	No.1	No.2	No.1	No.2	No.1	No.2	No.1	No.2			No.1	No.2
Radial Arteries												
Spiral Arteries												
Ascending Uterine arteries												
Image Quality	4	4	3	2	4	4	5	5			3	3
Subject No.	**22**		**23**		**24**		**25**				**26**	
Clinical Condition	IUGR		IUGR		IUGR		IUGR				IUGR	
GA (weeks)	35 + 2/7		33 + 3/7		27 + 1/7		34 + 4/7				34 + 5/7	
MRI scanner	3 T		3 T		3 T		3 T				3 T	
Placenta Position	A		A		A		A				P	
BMI	40.4		32.9		43.4		29.2				22	
Reader	No.1	No.2	No.1	No.2	No.1	No.2	No.1	No.2			No.1	No.2
Radial Arteries												
Spiral Arteries												
Ascending Uterine arteries												
Image Quality												

*Image quality (5-point score/2-point score): 5-point score: 1, non-diagnostic; 2, poor; 3, acceptable; 4, good; 5, excellent. 2-point score: 0, diagnostically not acceptable; 1, diagnostically acceptable.

Table 2.

MR parameters of MRA at 1.5 T and 3 T

1.5 T							
Sequence	**TR (ms)**	**TE (ms)**	**ΔTE (ms)/no of TE**	**FA (˚)**	**BW (Hz/px)**	**Resolution (mm × mm× mm)**	**Slice Number**
T2-HASTE	1400	152	x/1	180	355	1.17 × 1.17 × 5.0	22–36
MRA	23	5.6	x/1	50	245	0.56 × 0.56 × 3.0	22–36
3 T							
Sequence	**TR (ms)**	**TE (ms)**	**ΔTE (ms)/no of TE**	**FA (°)**	**BW (Hz/px)**	**Resolution (mm × mm × mm)**	**Slice Number**
T2-HASTE	1310	95	x/1	180	488	1.0 × 1.0 × 3.0	15–50
MRA	22	4.92	x/1	50	241	1.0 × 1.0 × 3.0	15–50
MRA (High Resolution)	22	4.92	x/1	50	241	0.5 × 0.5 × 3.0	15–50

Table 3.

Vessel visibility

Vessels Demonstrated	Umbilical Arteries		Umbilical Vein		Chorionic Vessels		Stem Vessels		Arcuate Arteries		Radial Arteries		Spiral Arteries		Hyrtl's Anastomosis		Uterine Arteries	
Reader	No.1	No.2	No.1	No.2	No.1	No.2	No.1	No.2	No.1	No.2	No.1	No.2	No.1	No.2	No.1	No.2	No.1	No.2
Number of Cases	26	26	26	26	25	26	22	25	26	26	24	20	24	23	2	2	14	21
Cases at 1.5 T (%)	42.3	42.3	42.3	42.3	44	42.3	41	44	42.3	42.3	41.7	45	41.7	47.8	100	100	42.9	42.9
κ	0.486																	

Table 4.

Image quality score

Reader	No.1	No.2
Image Quality Score (5 points)	3.8 ± 0.9 (2–5)	3.8 ± 1.0 (2–5)
κ	0.514	
Image Quality Score (2 Points)	1.9 ± 0.3 (1–2)	1.9 ± 0.3 (1–2)
κ	0.78	

5-point score: 1, nondiagnostic; 2, poor; 3, acceptable; 4, good; 5, excellent.

2-point score: 1, diagnostically not acceptable; 2, diagnostically acceptable.